NJC

Spectroelectrochemical properties of a Ru(II) complex with a thiazolo[5,4-d]thiazole triarylamine ligand†

Carol Hua,[a] Felix J. Rizzuto,[a] Xuan Zhang,[ab] Floriana Tuna,[c] David Collison[c] and Deanna M. D'Alessandro*[a]

A new bis-chelating ligand containing a triarylamine electron donor core fused with a thiazolo-thiazole electron acceptor, N,N'-(thiazolo[5,4-d]thiazole-2,5-diylbis(4,1-phenylene))bis(N-(pyridin-2-yl)pyridin-2-amine) (1) has been synthesised. This non-innocent ligand exhibits interesting electronic and spectral properties that can be tuned as a function of its redox state. In particular, modulation of the electronic state can be used to turn the fluorescence on and off. A dinuclear Ru(II) terpyridine complex, [Ru$_2$(tpy)$_2$Cl$_2$(1)](PF$_6$)$_2$ (2) was subsequently synthesised and the properties of each of the accessible redox states explored using in situ spectroelectrochemical techniques.

Introduction

In the quest for more renewable sources of energy, the development of devices capable of harnessing the energy provided by solar radiation is a subject of continuing extensive research efforts.[1–4] Ru(II) terpyridine (tpy) complexes, [Ru^{II}(tpy)]$^{2+}$, have been widely studied as a result of their favourable photoactive and charge transfer properties which facilitate the conversion of light into chemical energy.[5–8] Such complexes have also been employed as effective catalysts for a wide range of organic transformations.[9,10]

Towards the development of multifunctional systems, the combination of a [Ru^{II}(tpy)]$^{2+}$ species with a non-innocent redox-active ligand may provide a viable platform for new catalysts and light harvesting devices.[11,12] In this context, ligands containing donor and acceptor functionalities are particularly attractive owing to their potential to display multiple electronic states.[13–19] The use of triarylamines as redox-active moieties and electron donors has been extensively explored,[20–25] and their potential to undergo a one electron oxidation to form a radical cation[26,27] has enabled studies on organic mixed-valence compounds.[28–30] Meanwhile, thiazolo[5,4-d]thiazoles, consisting of two fused

heterocycles containing nitrogen and sulfur atoms are well-known acceptors in organic polymers.[31–34] It has previously been shown that the thiazolo-thiazole moiety is planar and capable of undergoing two sequential one electron reduction processes.[35,36]

Herein, the synthesis of a new donor–acceptor ligand comprising the triarylamine and thiazolo-thiazole moieties is described. To facilitate chelation of a metal centre, 2,2'-bipyridine N,N'-bidentate coordination sites were also introduced into N,N'-(thiazolo[5,4-d]thiazole-2,5-diylbis(4,1-phenylene))bis(N-(pyridin-2-yl)pyridin-2-amine) (1). Such donor–acceptor ligands have previously been shown to support strong electronic delocalisation over relatively large distances.[13,37] The new Ru(II) terpyridine complex, [Ru$_2$(tpy)$_2$Cl$_2$(1)](PF$_6$)$_2$ (2), was synthesised to investigate the potential multifunctionality. The electronic, spectral and fluorescence properties of both 1 and 2 have been investigated using in situ UV/Vis/NIR, EPR and fluorescence spectroelectrochemistry to investigate the physical properties as a function of the multiple accessible redox states.

Results and discussion

Synthesis and characterisation

The N,N'-(thiazolo[5,4-d]thiazole-2,5-diylbis(4,1-phenylene))bis-(N-(pyridine-2-yl)pyridin-2-amine) ligand (1) was synthesised as a bright yellow solid via a Goldberg reaction of 2,5-bis(4-bromo-phenyl)thiazolo[5,4-d]thiazole with excess 2,2'-dipyridylamine in 34% yield (Scheme 1a). The ruthenium complex 2 was synthesised by reaction of 1 and Ru(tpy)Cl$_3$ in the presence of N-methylmorpholine (NMM). The complex was isolated as a deep maroon solid in 34% yield after purification by column chromatography (Scheme 1b). The complex was characterised

[a] School of Chemistry, The University of Sydney, New South Wales 2006, Australia.
 E-mail: deanna.dalessandro@sydney.edu.au; Fax: +61 (2) 9351 3329;
  Tel: +61 (2) 9351 3777
[b] School of Chemistry and Chemical Engineering, Nanjing University, Nanjing, 210093, P. R. China
[c] School of Chemistry, University of Manchester, Manchester M13 9PL, UK
† Electronic supplementary information (ESI) available: ^{1}H–^{1}H COSY NMR, electrochemistry, fluorescence, UV/Vis/NIR and fluorescence spectroelectrochemistry. See DOI: 10.1039/c6nj02802k
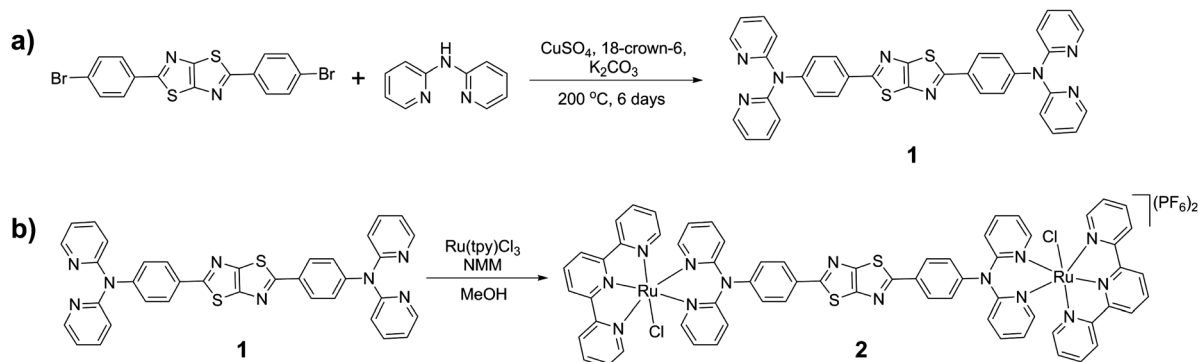
Scheme 1 Synthetic scheme for (a) **1** and (b) **2**.

by 1D and 2D NMR experiments, mass spectrometry and elemental analysis. The ^{1}H NMR spectrum in DMSO-d_6 revealed the C_2 symmetry of **2**: the complex displayed chemically equivalent signals for the two terpyridine ligands and the two halves of the central core of **1**. The two pyridyl rings on the triarylamine have chemically distinct resonances due to the asymmetric environment about the ruthenium metal centre, resulting from the symmetry-breaking coordination of the chloride ligand. The set of resonances corresponding to one of the triarylamine pyridyl rings was shifted significantly downfield when compared to those of the other triarylamine ring, reflecting the different proximities to the chloride or terpyridine ligands.

Probing the redox properties

The redox properties of **1** were investigated using solution state cyclic voltammetry in [(n-C$_4$H$_9$)$_4$N]PF$_6$/CH$_3$CN electrolyte. Three processes were observed in the anodic region at 0.035, 0.52 and 0.81 V $vs.$ Fc/Fc$^+$ (Fig. 1a). The first process at 0.035 V may be attributed to oxidation of the triarylamine pyridyl groups to pyridyl N-oxide species, which was supported by the absence of this redox process upon coordination of the ligand to a metal centre ($vide$ $infra$). The quasi reversible process at 0.52 V was assigned to the one electron oxidation of a single triarylamine core to its radical cation while the quasi reversible process at 0.81 V is consistent with a one electron oxidation of the adjacent triarylamine core.[26] In the cathodic region, four processes were observed at −1.24, −1.45, −2.04 and −2.37 V. The first two processes are due to reduction of the TzTz core while the third and fourth processes were attributed to reduction of the pyridyl rings. These processes are consistent with the previously reported 4-Py isomer of **1**.[13]

The cyclic voltammogram of **2** displayed two main processes in the anodic region (Fig. 1b). The reversible process at 0.32 V was assigned to the one electron oxidation of Ru(II) to Ru(III) while the quasi reversible process at 0.79 V corresponded well with the process in the ligand for the one electron oxidation of the triarylamine core to its radical cation. The absence of the peak at 0.036 V is consistent with the coordination of the pyridyl groups to the Ru^{2+} metal centre, which precludes their oxidation to the N-oxide species. A broad peak in the cathodic region of the CV was further explored by performing square
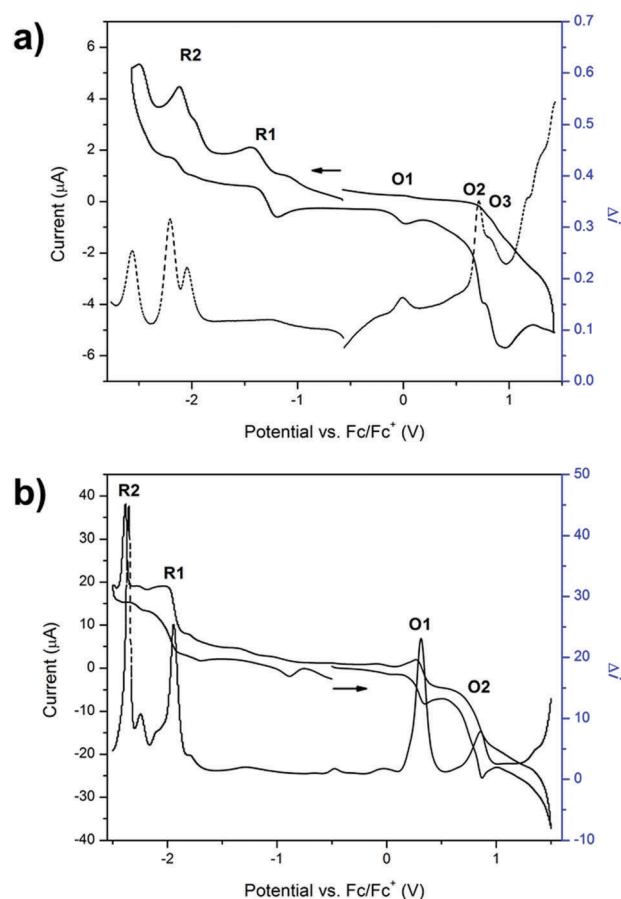

Fig. 1 Square wave (at an amplitude of 10 mV and frequency of 9 Hz) $vs.$ cyclic voltammograms at 100 mV s^{-1} in 0.1 M [(n-C$_4$H$_9$)$_4$N]PF$_6$/CH$_3$CN electrolyte of (a) **1** and (b) **2** where the arrow indicates the direction of the forward scan.

wave voltammetry, which showed two main processes in the cathodic region that were assigned to the two sequential one electron reductions of the TzTz core to its radical anion and dianion states (Fig. 1b). The reduction processes due to the free ligand lie outside the potential window afforded by acetonitrile due to stabilisation upon coordination to the ruthenium metal centre.

UV/Vis/NIR spectroelectrochemistry

The solution state UV/Vis/NIR spectrum of **1** in acetonitrile displayed two bands at 25 600 and 32 900 cm^{-1} which are assigned to $\pi \rightarrow \pi^*$ (LUMO–HOMO) transitions.[35,38] It was presumed that the molecular orbitals of **1** were similar to those of the analogous 4-pyridyl terminated system previously reported.[13] As a potential of −1.1 V was applied to **1** during the spectroelectrochemical experiment in [(n-C$_4$H$_9$)$_4$N]PF$_6$/CH$_3$CN electrolyte, the bands at 25 600 and 32 900 cm^{-1} increased due to reduction of the TzTz core to its radical anion (Fig. S5, ESI†).

Oxidation of **1** provided access to the radical cation state of the triarylamine moiety. As the potential was increased from 0.8 to 0.9 V, the bands at 25 600 and 32 900 cm^{-1} decreased (Fig. S5, ESI†). As the potential was further increased from 1.1 to 1.6 V, these bands further decreased in intensity, while a new band at 23 800 cm^{-1} formed (Fig. S5, ESI†). The decrease of the bands at 25 000 and 32 900 cm^{-1} resulted from the loss of electron density throughout the entire ligand due to the high degree of delocalisation in the system which was a consequence of the coplanarity of the TzTz and phenyl functionalities. This arrangement results in a highly delocalised HOMO over the ligand backbone, and a localised HOMO−1 on the triarylamine core.[13]

The UV/Vis/NIR spectrum of **2** exhibits three major features (Fig. 2a). The band at 19 000 cm^{-1} was assigned to the d $\rightarrow$ π^* MLCT transition between the terpyridine ligand and Ru^{2+} metal centre, and the bands at 25 000 and 32 000 cm^{-1} are attributed to the $\pi \rightarrow \pi^*$ transitions of the aromatic moieties in the terpyridine ligands and in the bridging ligand **1**.

The solution state UV/Vis/NIR spectroelectrochemical experiment on **2** in [(n-C$_4$H$_9$)$_4$N]PF$_6$/CH$_3$CN electrolyte displayed several processes upon application of a positive potential. At 1.0 V, a decrease in the MLCT band at 19 600 cm^{-1} was observed, corresponding to a loss of electron density from the metal centre due to oxidation of the Ru(II) centre to Ru(III) (Fig. 2a). The decrease in intensity of the band at 25 500 cm^{-1} was due to electron density being transferred towards the ruthenium centre, resulting in a depopulation of the LUMO. As the potential was further increased from 1.3 to 1.6 V, a band at 31 200 cm^{-1} appeared as the band at 25 500 cm^{-1} continued to decrease (Fig. 2c). The original spectrum of the complex was regained upon decreasing the potential to 0 V, indicating that the processes were spectrally reversible (Fig. 2d).

As the potential was changed from −1.05 to −1.5 V, the bands at 25 200 and 31 390 cm^{-1} decreased in intensity, while a
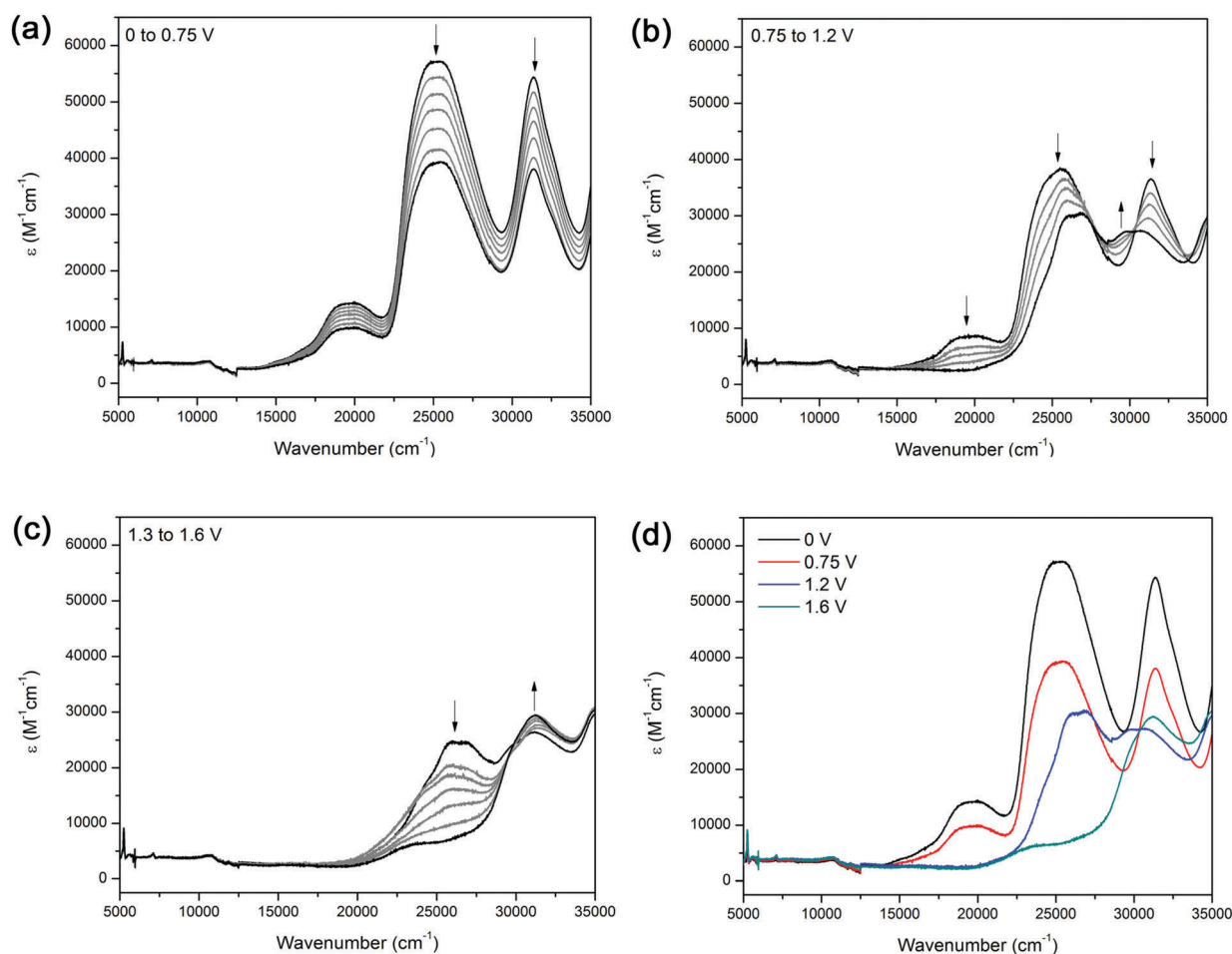

Fig. 2   Solution state spectroelectrochemistry on **2** in [(n-C$_4$H$_9$)$_4$N]PF$_6$/CH$_3$CN electrolyte over the potential range of (a) 0 to 0.75 V, (b) 0.75 to 1.2, (c) 1.3 to 1.6 V and (d) summary of the changes in the absorption spectrum as a function of potential applied.

narrow band at 21 300 cm^{-1} appeared, presumably due to reduction of the thiazolo[5,4-*d*]thiazole moiety (Fig. S6, ESI†). The blue shift of the MLCT band at 19 000 to 21 300 cm^{-1} may arise from the increase in electron density on the ligand backbone.

EPR spectroelectrochemistry

EPR spectroelectrochemical experiments were conducted on **1** in [(*n*-C$_4$H$_9$)$_4$N]PF$_6$/CH$_3$CN electrolyte (Fig. 3a). An EPR signal at *g* = 2.004 was obtained upon the application of a potential of 1.7 V, which corresponds to the formation of the triarylamine radical cation.

The solution-state EPR spectroelectrochemical experiment on **2** in [(*n*-C$_4$H$_9$)$_4$N]PF$_6$/CH$_3$CN electrolyte at 240 K yielded a signal at *g* = 2.002 with a 1:1:1 hyperfine pattern at 1.8 V, where the radical is primarily localised on the triarylamine nitrogen centre and has a hyperfine coupling value of 28 MHz (Fig. 3a). The hyperfine information of the signal was lost upon warming the reaction mixture to room temperature to yield one broad peak. This is due to the faster rate of molecular tumbling at higher temperatures, whereas the lower temperatures resulted in slower molecular movement, allowing the hyperfine coupling to be elucidated. A colour change from deep red to light yellow was observed during the experiment, corresponding to formation of the Ru^{3+} species and subsequently, oxidation of the triarylamine to its radical cation (Fig. 3b).

Redox state dependent fluorescence

A light blue fluorescence band was observed for **1** in acetonitrile at 480 nm (20 900 cm^{-1}) upon excitation into the $\pi \rightarrow \pi^*$ transition at 390 nm (25 600 cm^{-1}) with a Stoke's shift of 216 nm (Fig. S7, ESI†). **2** displayed a fluorescence peak at 470 nm (21 280 cm^{-1})

upon excitation at 400 nm (25 000 cm^{-1}) into the ligand $\pi \rightarrow \pi^*$ transition (Fig. S7, ESI†). When the other bands in the absorption spectrum of the metal complex were excited (320 and 512 nm), no fluorescence peaks were observed. These results may suggest a high quantum yield for **1**, and a low quantum yield for **2**.

The fluorescence was quenched upon oxidation of Ru^{2+} to Ru^{3+} in **2** with NOPF$_6$ (0.87 *vs.* Fc/Fc$^+$) in acetonitrile.[39] As shown from the chemical oxidation of **2**, the fluorescence is able to be tuned as a function of the redox state. In order to verify that the fluorescence quenching observed *ex situ* from the chemically oxidised species was due to the formation of the triarylamine radical cation and not due to external environmental factors, *in situ* fluorescence spectroelectrochemical experiments were performed in [(*n*-C$_4$H$_9$)$_4$N]PF$_6$/CH$_3$CN electrolyte on both **1** and **2** (Fig. S8 and S9, ESI†).

In **1**, increasing the potential to 1.5 V resulted in a decrease of the fluorescence peaks at 504 and 533 nm, corresponding to the formation of one of the triarylamine radical cation centres in the ligand. An additional increase in the potential from 1.7 to 2.0 V, led to a decrease in the fluorescence, corresponding to the oxidation of the second triarylamine core (Fig. S8, ESI†).

Similar trends for the *in situ* fluorescence spectroelectrochemical experiment were observed for **2** (Fig. S9, ESI†). Upon oxidation, a decrease in the fluorescence band at 475 nm was observed due to formation of the triarylamine radical cation, while application of a reductive potential of −1.0 V resulted in the (re)formation of the band, corresponding to the regeneration of the neutral state. The fluorescence behaviour of the ruthenium complex can therefore be attributed to predominantly ligand based processes.

Conclusions

The combination of the electron donating triarylamine core with the electron accepting thiazolo-thiazole moiety within ligand **1** and Ru(ii) complex **2** has resulted in a versatile donor–acceptor system. The accessibility of the different redox states has been demonstrated through spectroelectrochemical experiments, with the properties of each redox state characterised. The tunability of the complex's fluorescence properties as a function of redox state may lend to its application in photoactive and catalytic processes.

Experimental

General considerations and synthetic procedures

All chemicals and solvents were used as obtained without further purification. 2,2′-Dipyridylamine,[40] Ru(tpy)Cl$_3$[41,42] and 2,5-bis(4-bromophenyl)thiazolo[5,4-*d*]thiazole[43,44] were synthesised according to literature procedures. For experiments requiring dry solvents, acetonitrile was dried over CaH$_2$ and methanol was dried over magnesium/magnesium methoxide before being distilled under nitrogen. Toluene was obtained from a PuraSolv solvent purification system and stored over activated 4 Å molecular sieves.

Solution state ^{1}H and ^{13}C{^{1}H} NMR spectra were recorded on either a Bruker AVANCE300 or AVANCE500 spectrometer
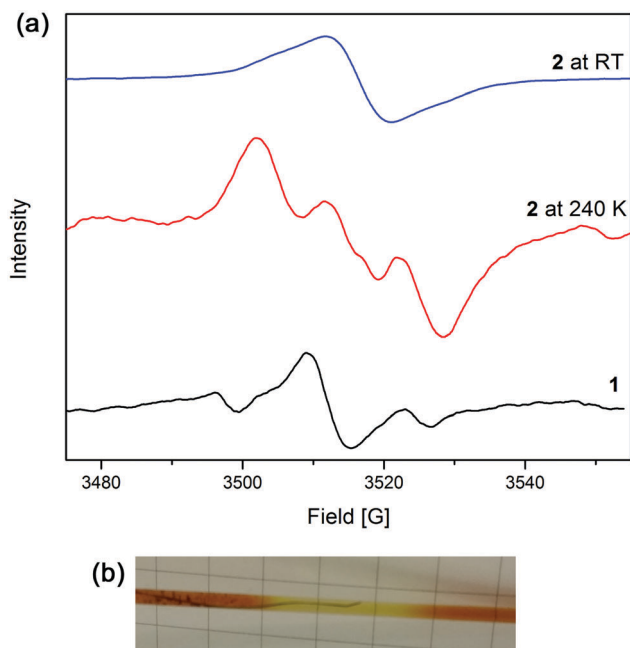

Fig. 3 (a) EPR spectra in [(*n*-C$_4$H$_9$)$_4$N]PF$_6$/CH$_3$CN electrolyte of **1** and **2** at 240 K and room temperature and (b) photo of the EPR cell with electrodes during the experiment showing the colour change from deep red to yellow.

operating at 300, 500 MHz for ^{1}H and 75, 125 MHz for ^{13}C, respectively. ^{1}H and ^{13}C NMR chemical shifts were referenced internally to residual solvent resonances. Spectra were recorded at 298 K and chemical shifts (δ), with uncertainties of ±0.01 Hz for ^{1}H and ±0.05 Hz for ^{13}C are quoted in ppm. Coupling constants (J) are quoted in Hz and have uncertainties of ±0.05 Hz for ^{1}H–^{1}H. Deuterated solvents were obtained from Cambridge Stable Isotopes and used as received. Mass spectrometry was carried out at the mass spectrometry analysis facility at the University of Sydney on a Finnigan LCQ mass spectrometer. Microanalyses were carried out at the Chemical Analysis Facility – Elemental Analysis Service in the Department of Chemistry and Biomolecular Science at Macquarie University, Australia.

N,N'-(Thiazolo[5,4-d]thiazole-2,5-diylbis(4,1-phenylene))bis(N-(pyridine-2-yl)pyridin-2-amine) (1)

2,2′-Dipyridylamine (430 mg, 2.50 mmol), 2,5-bis(4-bromophenyl)-thiazolo[5,4-d]thiazole (450 mg, 1.00 mmol), anhydrous potassium carbonate (690 mg, 5.00 mmol), anhydrous copper sulfate (150 mg, 0.900 mmol), 18-crown-6 (36.0 mg, 0.150 mmol) and diphenyl ether (10.0 mL) were heated at 200 °C under nitrogen for 48 h. The reaction mixture was cooled to room temperature before water (20.0 mL) was added. The aqueous layer was extracted with dichloromethane (3 × 50 mL), and the organic layer dried over Na_2SO_4. The solvent was removed under reduced pressure and the residue purified by silica gel column chromatography (using an elution gradient of 20:1 CH_2Cl_2:Et_3N to 20:1:1 CH_2Cl_2:Et_3N:MeOH) to yield the pure product as a yellow powder (180 mg, 34%), m.p. >260 °C. ^{1}H NMR (300 MHz, d_6-DMSO): 8.31 (dd, $^3J_{H-H}$ = 4.8 Hz, $^4J_{H-H}$ = 1.2 Hz, 4H, H10), 8.02–7.97 (m, 4H, H9), 7.79–7.73 (m, 4H, H8), 7.20 (d, $^3J_{H-H}$ = 8.7 Hz, 4H, H4), 7.12 (dd, $^3J_{H-H}$ = 7.3, $^4J_{H-H}$ = 4.9 Hz, 4H, H7), 7.06 (d, $^3J_{H-H}$ = 8.3 Hz, 4H, H5) ppm. ^{13}C{^{1}H} NMR (75 MHz, d_6-DMSO): δ 168.0 (C2), 157.2 (C7), 150.1 (C1), 148.5 (C3), 147.5 (C10), 138.3 (C9), 129.0 (C4), 127.3 (C6), 126.2 (C9), 119.3 (C8), 117.7 (C5) ppm. ESI-MS (ESI$^+$, MeOH): 633.00 (calculated [M + H]$^+$ = 633.16, 100%) amu. HR-MS (MeOH): found 655.14559 (calculated [M + Na]$^+$ = 655.14576) amu. Elemental analysis; found: C, 68.46, H, 3.31, N, 17.75, S, 10.04%. Calculated for $C_{36}H_{24}N_8S_2$: C, 68.33, H, 3.82, N, 17.71, S, 10.13%.

[Ru$_2$(tpy)$_2$Cl$_2$(1)](PF$_6$)$_2$ (2)

Ru(tpy)Cl$_3$ (139 mg, 0.316 mmol) and 1 (100 mg, 0.158 mmol) were suspended in dry methanol (80.0 mL) and N-methylmorpholine (5.0 mL) was added. The green suspension was heated at reflux under nitrogen for 24 hours to yield a deep green solution, then cooled to room temperature. The solvent was reduced and a saturated solution of KPF$_6$ in water was added to the reaction mixture to yield a dark purple-brown precipitate. The solid was isolated by filtration and washed with water before being dried. The crude product was purified by a silica gel column (19:1:0.1 CH$_3$CN:H$_2$O:KNO$_3$ (sat. solution in water)), before the product fractions were combined and a saturated solution of NH$_4$PF$_6$ in water added to yield the precipitation of a dark red solid. The solid was dried under vacuum to yield the product (77.0 mg, 34%). ^{1}H NMR (500 MHz, d_6-DMSO): 9.75 (d, $^3J_{H-H}$ = 4.5 Hz, 2H, H8a),

8.76 (d, $^3J_{H-H}$ = 8.5 Hz, 4H, H18), 8.67 (d, $^3J_{H-H}$ = 8.0 Hz, 4H, H15), 8.42 (td, $^3J_{H-H}$ = 8.0 Hz, $^4J_{H-H}$ = 1.5 Hz, 2H, H10a), 8.28 (d, $^3J_{H-H}$ = 8.0 Hz, 2H, H11a), 8.17 (t, $^3J_{H-H}$ = 8.0 Hz, 2H, H19), 7.98 (d, $^3J_{H-H}$ = 6.0 Hz, 4H, H12), 7.96 (t, $^3J_{H-H}$ = 7.5 Hz, 4H, H13), 7.91–7.88 (m, 6H, H4 and H9a), 7.75 (td, $^3J_{H-H}$ = 7.5 Hz, $^4J_{H-H}$ = 1.5 Hz, 2H, H9), 7.63 (d, $^3J_{H-H}$ = 8.0 Hz, 2H, H8), 7.15 (t, $^3J_{H-H}$ = 6.5 Hz, 4H, H14), 6.98 (d, $^3J_{H-H}$ = 8.0 Hz, 4H, H5), 6.96 (d, $^3J_{H-H}$ = 6.0 Hz, 2H, H11), 6.92 (t, $^3J_{H-H}$ = 8.0 Hz, 2H, H10) ppm. ^{13}C{^{1}H} NMR (125 MHz, d_6-DMSO): δ 167.6 (C2), 158.7 (C16), 158.6 (C17), 156.7 (C11), 154.0 (C7a), 152.6 (C13), 150.83 (C7), 149.9 (C1), 146.3 (C3), 139.4 (C10a), 138.5 (C9), 136.9 (C14), 133.72 (C19), 127.7 (C4), 127.3 (C6), 126.5 (C12), 124.1 (C11a), 123.8 (C9a), 123.7 (C8a, C8, C10), 123.5 (C15), 122.7 (C18), 116.3 (C5) ppm. ESI-MS (ESI$^+$, MeOH): 685.93 (calculated [M-2PF$_6$]$^{2+}$ = 686.045, 100%) amu. Elemental analysis; found: C, 48.77, H, 3.45, N, 11.54, S, 5.04. Calculated for $C_{69}H_{54}Cl_2F_{12}N_{14}P_2Ru_2S_2$: C, 48.57, H, 3.19, N, 11.49, S, 5.10%.

Physical measurements

Mass spectrometry. Low resolution electrospray ionisation (ESI) mass spectra were acquired in a solution of acetonitrile or methanol with a 100 μL min^{-1} flow rate on a Finnegan LCQ MS detector. Spectra were collected over the mass range m/z = 50 to 2000. An ESI spray voltage of 5 kV was applied with a heated capillary temperature of 200 °C and a nitrogen sheath gas pressure of 60 psi.

Infrared spectroscopy (DRIFTS). FT-IR was performed on samples in a KBr matrix over the range 4000–400 cm^{-1} on a Bruker Tensor 27 FT-IR spectrometer with a resolution of 4 cm^{-1}.

Solution state UV/Vis/NIR spectroscopy. Solution state UV/Vis/NIR spectra were obtained over the range of 3500–35 000 cm^{-1} using a CARY5000 Spectrophotometer interfaced with Varian WinUV software. The baseline was taken with the solvent that the sample was to be dissolved in prior to measurement of the sample of interest. A 3 mL (1 cm pathlength) quartz cuvette was used.

Solution state electrochemistry. Solution state electrochemical measurements were performed using a Bioanalytical Systems BAS 100A Electrochemical Analyser. Argon was bubbled through the electrolyte solution (0.1 M [(n-C$_4$H$_9$)$_4$N]PF$_6$ in either CH$_3$CN or CH$_2$Cl$_2$) containing a small sample of the compound of interest prior to the start of the experiment. The cyclic voltammograms (CVs) and square wave voltammograms (SW) were recorded using a glassy carbon working electrode (1.5 mm diameter), a platinum wire auxiliary electrode and an Ag/Ag$^+$ wire quasi-reference electrode. Ferrocene was added as an internal standard upon completion of each experiment. All potentials are quoted in V $versus$ Fc$^+$/Fc.

Solution state spectroelectrochemistry (UV/Vis/NIR). Solution state UV/Vis/NIR spectroelectrochemistry over the range of 3500–35 000 cm^{-1} was performed using a CARY5000 spectrophotometer interfaced with Varian WinUV software. In the solution state, the absorption spectra of the electrogenerated species were obtained in $situ$ by the use of an Optically Semi-Transparent Thin-Layer Electrosynthetic (OSTLE) cell, path length 0.65 mm, mounted in the path of the spectrophotometer. Solutions for the spectroelectrochemical experiment contained

0.1 M $[(n\text{-}C_4H_9)_4N]PF_6/CH_3CN$ supporting electrolyte and *ca.* 1 mM of the compound. Appropriate potentials were applied by using an eDAQ e-corder 410 potentiostat and the current was carefully monitored throughout the electrolysis. By this method, the electrogenerated species were obtained *in situ*, and their absorption spectra were recorded at regular intervals throughout the electrolysis. The attainment of a steady-state spectrum and the decay of the current to a constant minimum at a potential appropriately beyond $E_{1/2}$ (for the redox process in question) was indicative of the complete conversion of the starting material.

Solution state spectroelectrochemistry (EPR). The procedure and cell set up used were as described previously.[45] A three-electrode assembly based on simple narrow wires (A–M Systems) as electrodes where Teflon coated platinum (0.20 and 0.13 mm coated and uncoated diameters, respectively) and silver wires (0.18 and 0.13 mm coated and uncoated diameters, respectively) were used for the working and quasi-reference electrodes respectively, and a naked platinum wire (0.125 mm) as the counter electrode. The bottom 1 cm of the Teflon coated wires were stripped (using an Eraser International Ltd, RT2S fine wire stripper). The working electrode was positioned lowest such that the redox product of interest is generated at the bottom of the tube and well separated from the counter electrode. The naked platinum wire counter electrode ensures a greater surface area than the working electrode, while the Teflon coating on the working and reference electrodes prevents short-circuiting. The electrodes were soldered to a narrow three-core microphone wire. The cell used was made by flame sealing the tip of a glass pipette. The potential was controlled with a portable μAutolab II potentiostat and the EPR spectra obtained using an EMX Micro X-band EPR spectrometer with 1.0 T electromagnet.

Solution state fluorescence spectroscopy. Fluorescence data were collected on a Cary Varian Eclipse Fluorescence Spectrophotometer. Excitation wavelengths were determined by UV/Vis/NIR spectra, and maximum excitations deduced from emission-excitation spectra. The scan rate used for all measurements was 120 nm min^{-1} with a 1 nm data interval. The fluorescence spectrum of the species of interest was obtained from a solution of the compound in acetone or acetonitrile in a quartz cuvette (1 cm × 1 cm × 1 cm) with excitation at 380 nm, the emission spectrum obtained from 400–750 nm and slit widths of 2.5 mm which were used for both excitation and emission.

Solution state spectroelectrochemistry (fluorescence). The Optically Semi-Transparent Thin-Layer Electrosynthetic (OSTLE) cell used for the solution state UV/Vis/NIR spectroelectrochemical experiment, path length 0.65 mm, was adapted for use in a fluorimeter by placing the OSTLE cell perpendicular to the excitation and emission windows. Solutions for the spectroelectrochemical experiment contained 0.1 M $[(n\text{-}C_4H_9)_4N]PF_6/CH_2Cl_2$ or $[(n\text{-}C_4H_9)_4N]PF_6/CH_3CN$ supporting electrolyte and *ca.* 1 μM of the compound (dependent on the fluorescence intensity). Appropriate potentials were applied by using an eDAQ e-corder 410 potentiostat and the current was carefully monitored throughout the electrolysis. The electrogenerated species were obtained *in situ*, and their emission spectra were recorded at a scan rate of 100 nm min^{-1} at regular intervals throughout the electrolysis.

Notes and references

1 M. C. So, G. P. Wiederrecht, J. E. Mondloch, J. T. Hupp and O. K. Farha, *Chem. Commun.*, 2015, **51**, 3501–3510.
2 A. Bahadori and C. Nwaoha, *Renewable Sustainable Energy Rev.*, 2013, **18**, 1–5.
3 T. G. Deepak, G. S. Anjusree, S. Thomas, T. A. Arun, S. V. Nair and A. Sreekumaran Nair, *RSC Adv.*, 2014, **4**, 17615–17638.
4 T. Ameri, P. Khoram, J. Min and C. J. Brabec, *Adv. Mater.*, 2013, **25**, 4245–4266.
5 J. Choi, H. M. Nguyen, S. Yoon, N. Kim, J.-W. Oh and F. S. Kim, *Mol. Cryst. Liq. Cryst.*, 2014, **600**, 22–27.
6 P. Hrobárik, V. Hrobáriková, I. Sigmundová, P. Zahradník, M. Fakis, I. Polyzos and P. Persephonis, *J. Org. Chem.*, 2011, **76**, 8726–8736.
7 A. O. Adeloye and P. A. Ajibade, *Molecules*, 2014, **19**, 12421–12460.
8 L. Hammarstroem and O. Johansson, *Coord. Chem. Rev.*, 2010, **254**, 2546–2559.
9 J. J. Concepcion, J. W. Jurss, M. K. Brennaman, P. G. Hoertz, A. O. T. Patrocinio, N. Y. Murakami Iha, J. L. Templeton and T. J. Meyer, *Acc. Chem. Res.*, 2009, **42**, 1954–1965.
10 A. Winter, G. R. Newkome and U. S. Schubert, *ChemCatChem*, 2011, **3**, 1384–1406.
11 W. Kaim and J. Fiedler, *Chem. Soc. Rev.*, 2009, **38**, 3373–3382.
12 M. Venturi, *Lect. Notes Chem.*, 2012, **78**, 209–225.
13 F. J. Rizzuto, T. B. Faust, B. Chan, C. Hua, D. M. D'Alessandro and C. J. Kepert, *Chem. – Eur. J.*, 2014, **20**, 17597–17605.
14 D. M. D'Alessandro, *Chem. Commun.*, 2016, **52**, 8957–8971.
15 C. F. Leong, B. Chan, T. B. Faust and D. M. D'Alessandro, *Chem. Sci.*, 2014, **5**, 4724–4728.
16 C. L. Ramírez, C. N. Pegoraro, O. Filevich, A. Bruttomeso, R. Etchenique and A. R. Parise, *Inorg. Chem.*, 2012, **51**, 1261–1268.
17 C.-J. Yao, R.-H. Zheng, Q. Shi, Y.-W. Zhong and J. Yao, *Chem. Commun.*, 2012, **48**, 5680–5682.
18 H.-J. Nie, W.-W. Yang, J.-Y. Shao and Y.-W. Zhong, *Dalton Trans.*, 2016, **45**, 10136–10140.
19 C.-J. Yao, Y.-W. Zhong and J. Yao, *Inorg. Chem.*, 2013, **52**, 4040–4045.
20 C. Hua, B. Chan, A. Rawal, F. Tuna, D. Collison, J. M. Hook and D. M. D'Alessandro, *J. Mater. Chem. C*, 2016, **4**, 2535–2544.
21 C. Hua, P. Turner and D. M. D'Alessandro, *Dalton Trans.*, 2015, **44**, 15297–15303.
22 C. Hua and D. M. D'Alessandro, *Supramol. Chem.*, 2015, **27**, 792–797.
23 C. Hua, A. Rawal, T. B. Faust, P. D. Southon, R. Babarao, J. M. Hook and D. M. D'Alessandro, *J. Mater. Chem. A*, 2014, **2**, 12466–12474.

24 C. Hua and D. M. D'Alessandro, *CrystEngComm*, 2014, **16**, 6331–6334.

25 C. Hua, P. Turner and D. M. D'Alessandro, *Dalton Trans.*, 2013, **42**, 6310–6313.

26 S. Amthor, B. Noller and C. Lambert, *Chem. Phys.*, 2005, **316**, 141–152.

27 C. Lambert and G. Nöll, *J. Am. Chem. Soc.*, 1999, **121**, 8434–8442.

28 A. Heckmann and C. Lambert, *Angew. Chem., Int. Ed.*, 2012, **51**, 326–392.

29 C. Lambert and G. Nöll, *Synth. Met.*, 2003, **139**, 57–62.

30 C. Lambert, G. Noll and J. Schelter, *Nat. Mater.*, 2002, **1**, 69–73.

31 I. Osaka, R. Zhang, J. Liu, D.-M. Smilgies, T. Kowalewski and R. D. McCullough, *Chem. Mater.*, 2010, **22**, 4191–4196.

32 T. W. Lee, N. S. Kang, J. W. Yu, M. H. Hoang, K. H. Kim, J.-I. Jin and D. H. Choi, *J. Polym. Sci., Part A: Polym. Chem.*, 2010, **48**, 5921–5929.

33 J. Roncali, *Macromol. Rapid Commun.*, 2007, **28**, 1761–1775.

34 S. Ando, J.-I. Nishida, H. Tada, Y. Inoue, S. Tokito and Y. Yamashita, *J. Am. Chem. Soc.*, 2005, **127**, 5336–5337.

35 M. R. Pinto, Y. Takahata and T. D. Z. Atvars, *J. Photochem. Photobiol., A*, 2001, **143**, 119–127.

36 S. Van Mierloo, S. Chambon, A. E. Boyukbayram, P. Adriaensens, L. Lutsen, T. J. Cleij and D. Vanderzande, *Magn. Reson. Chem.*, 2010, **48**, 362–369.

37 F. J. Rizzuto, C. Hua, B. Chan, T. B. Faust, A. Rawal, C. F. Leong, J. M. Hook, C. J. Kepert and D. M. D'Alessandro, *Phys. Chem. Chem. Phys.*, 2015, **17**, 11252–11259.

38 A. Brillante, B. Samori, C. Stremmenos and P. Zanirato, *Mol. Cryst. Liq. Cryst.*, 1983, **100**, 263.

39 N. G. Connelly and W. E. Geiger, *Chem. Rev.*, 1996, **96**, 877–910.

40 P. J. Zapf, R. L. LaDuca, R. S. Rarig, K. M. Johnson and J. Zubieta, *Inorg. Chem.*, 1998, **37**, 3411–3414.

41 D. Hvasanov, A. F. Mason, D. C. Goldstein, M. Bhadbhade and P. Thordarson, *Org. Biomol. Chem.*, 2013, **11**, 4602–4612.

42 B. P. Sullivan, J. M. Calvert and T. J. Meyer, *Inorg. Chem.*, 1980, **19**, 1404–1407.

43 S. Hisamatsu, H. Masu, I. Azumaya, M. Takahashi, K. Kishikawa and S. Kohmoto, *Cryst. Growth Des.*, 2011, **11**, 5387.

44 J. R. Johnson and R. Ketcham, *J. Am. Chem. Soc.*, 1960, **82**, 2719.

45 Y. Liu, J.-R. Li, W. M. Verdegaal, T.-F. Liu and H.-C. Zhou, *Chem. – Eur. J.*, 2013, **19**, 5637–5643.